UC Berkeley
Envelope Systems

Title
A simulation-based design analysis for the assessment of indoor comfort under the effect of solar radiation

Permalink
https://escholarship.org/uc/item/5vb3x9d6

Authors
Zani, Andrea
Richardson, Henry D
Tono, Alberto
et al.

Publication Date
2019-04-07

Copyright Information

Peer reviewed

A simulation-based design analysis for the assessment of indoor comfort under the effect of solar radiation

Andrea Zani[1, 4], Henry David Richardson[2], Alberto Tono[3], Stefano Schiavon[4] and Edward Arens[4]

[1] Eckersley O'Callaghan	[2] WattTime	[3] Hok	[4] CBE, UC Berkeley
San Francisco, USA	Oakland, USA	San Francisco, USA	Berkeley, USA
sanfrancisco@eocengineers.com	info@watttime.com	sf@hok.com	cbe@berkeley.edu

ABSTRACT

One of the drivers of sustainable design is to maximize daylight across the floor plan in order to decrease electric energy consumption and create more productive and healthy working spaces. However, uncontrolled incoming solar radiation can lead to significant visual and thermal comfort issues. In particular, solar radiation landing on occupants can create thermal discomfort that the HVAC system cannot compensate for, thereby causing intolerable conditions for users close to the façade.

We aim to present a new climate-based annual framework, based on ASHRAE 55 appendix C (2017), to assess radiant discomfort across a space due to direct solar radiation. The framework is calculated using the hourly effective radiant field (ERF) and delta Mean Radiant Temperature (ΔMRT) across the indoor space. The Radiance-based framework coupled with the proposed Annual Radiation Discomfort metric (ARD) provides designers a robust method to assess the performance of complex fenestration systems (CFS) at reducing potential thermal discomfort caused by incoming shortwave radiation.

Author Keywords

Solar radiation; Thermal comfort; Radiance; Complex Fenestration System; Annual Radiation Discomfort index.

1   INTRODUCTION

Controlling incoming solar radiation is one of the main goals for sustainable designers to minimize glare and cooling loads and maximize thermal comfort and usable daylight.

Uncontrolled solar radiation entering the building can introduce significant problems related to visual and thermal comfort. Thermal issues include to heat gains that must be removed by energy-intensive air conditioning, the risk of overcooling from attempting to compensate for the strong local heat gains in sunlit areas and solar radiation landing on occupants directly affects their thermal comfort. However, the third issue has been often overlooked because of the lack of guidelines and the complexity of the problem. The main thermal comfort standards, such as ASHRAE Standard 55 (ASHRAE 2004) or ISO Standard 7730 (ISO 2015), historically did not even mention shortwave solar radiation in their comfort prediction or evaluation procedures because they were developed assuming occupants would not be exposed to direct solar radiation inside the buildings. Only recently has ASHRAE 55-2017 adopted a method defined by the Center for the Built Environment to calculate discomfort due to shortwave radiation.

In modern glass office buildings where the window-to-wall ratio (WWR) is often close to 80% for aesthetic reasons and to maximize views, the critical design area for thermal comfort is the daylit perimeter zone [10] because of the potential for solar radiation landing on occupants. As proven in different publications [2, 12], shortwave incoming radiation can be the most influential component driving human comfort. The solar radiation that hits the occupant causes a substantial temperature offset which is often beyond the HVAC system's corrective capacity. Even if the HVAC mechanical cooling were capable of counteracting the discomfort of the sunlit occupant, the spatial and temporal variability of the sunlit areas exceeds that of typical HVAC zonal control, and the system will overcool the (usually more numerous) occupants in non-sunlit areas. Different surveys show [9, 10] that in many buildings situated in climates with high solar irradiance throughout the year and characterized by transparent facades the daylit perimeter area is unoccupied or the occupants are forced to deploy the shading for most of the day because of intolerable thermal conditions created by the excess of incoming solar radiation. In addition to the direct effect on human thermal comfort and productivity [1, 18], over deployed shading and the unused floor area near windows has profound impacts on daylight, energy building performance [3, 13] and economic efficiency. For these reasons, in order to help designers account for the direct influence of solar radiation on thermal comfort, ASHRAE 55-2017 Appendix C introduced two approaches to calculate the shortwave MRT.

ASHRAE 55-2017 includes two approaches for estimating the comfort condition when direct beam solar radiation hits the occupant. 1. Prescriptive approach: assume an MRT equal to 2.8 °C above the average air temperature which is

applicable only when prescribed conditions are met including: glazing elements' U-value, maximum outside temperature, maximum window size, blind solar transmission, and spatial room requirements (distance from the facade). 2. Performance approach based on the work of Arens et al. [2]: first compute the long wave and shortwave MRT and then sum the two quantities in order to obtain the adjusted MRT. As explained in the standard, the shortwave MRT is a function of the context, direct and indirect solar transmittance of the fenestration system, occupant position and posture, body exposure, sun position and irradiance value and clothing absorptivity. In the last couple of years, the ASHRAE full calculation method has been implemented in different tools such as SolarCal module of the CBE Thermal Comfort Tool [8] and Ladybug Comfort Component [11, 14] and a new workflow based on Radiance and EnergyPlus [20] that overcome some limitations of previous tools by adding features such as annual evaluations, automatic sky vault estimation, and projected fraction of a representative person exposed to direct beam sunlight in cases with complex fenestration systems (CFS). Compared to a "non-geometric" approach implemented in Trnsys [19] or Ladybug for grid calculation [11], manikin-based method allows to fully capture the distribution and intensity of the incoming radiation on the body. Particular improvements have been noticed [20] for highly directional solar shading system, where only portions of the body are hit by direct radiation. Currently, in architectural practice, facades and floor design solutions are often driven by preliminary daylight and solar heat gain analyses using metrics such as Daylight Autonomy (DA) [15], Useful Daylight Illuminance (UDI) [16], and Annual Sunlight Exposure (ASE). This leads to the question of whether current daylight performance metrics are well suited for the evaluation of the effect of solar radiation on human comfort. The most obvious limitation is that all the metrics are based on illuminance values or targeted toward HVAC system sizing (quantity of solar heat gain). This demonstrates that a thermal-comfort-focused, simulation-based framework and metric is missing from the design process.

In this paper, we present a new simulation framework, based on Zani's paper [20], for predicting the variation in indoor thermal comfort of occupants exposed to solar radiation across the floor plan by computing the change in MRT as a function of the area exposed and of the intensity of solar radiation. Furthermore, we present a new metric to assess the number of annual hours of discomfort caused by solar radiation and their discomfort intensity. Finally, we test the framework and the metric with three different facade system and determine their effect on the Predicted Mean Vote (PMV) near the facade.

2 METHOD

The climate-based shortwave radiation comfort framework used here allows the evaluation of the effect of direct solar radiation on human thermal comfort across indoor spaces over a one-year period. It consists of a refined and extended workflow based on a validated Radiance and EnergyPlus simulations approach [20] and a novel metric: the Annual Radiation Discomfort (ARD) index (defined in section 2.4). The scope of the new framework is to provide meaningful insight on how well a facade system controls incoming solar radiation to guarantee the thermal comfort of the occupants. It is intended to help quantify the frequency and intensity of the thermal discomfort caused by solar radiation during the year in a commercial building.

2.1 Simulation Framework

The simulation framework is divided into four main components as shown in Figure 1. First, using Rhinoceros 3D and Grasshopper, we create a series of manikins across the space and the subject scene. Second, we import the scene and manikin grid, previously generated, into Radiance. These files were used to calculate the incident solar radiation on the manikins employing the 2-phase Daylight Coefficient method. Third, we compute the long wave MRT for the each specific user's positions near the façade through EnergyPlus (E+). Finally, we analyze the raw output files using a custom Python script to obtain the hourly shortwave MRT and determine the adjusted MRT by coupling the results from the Radiance radiation analysis with E+ thermal analysis. The Annual Radiation Discomfort index is computed directly from the shortwave MRT without accounting for the effect of the long wave MRT. Given the magnitude of the effect of shortwave radiation landing on the occupants, long wave radiation can be overlooked in early design.
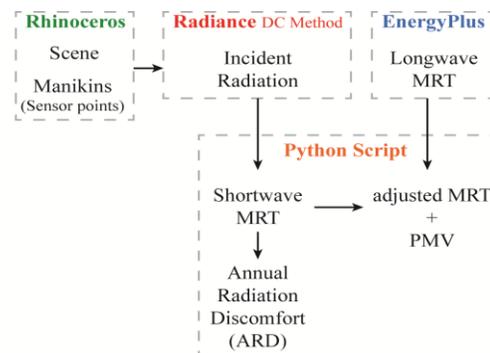

Figure 1. Simulation workflow. In colors the software used and in black each output obtained.

Incident Radiation - Radiance Calculation

The main change introduced in the framework is the automated hourly calculation for the entire year of the incoming radiation falling on the users across the space using Radiance. In particular, given the high resolution required to capture the amount of radiation in a specific portion of the manikin, we selected a modified version of the Daylight Coefficient . This method, in contrast with the traditional method where the luminance of the sun is attributed to the three patches closest to the sun, considers the exact position of the solar disc along the analemma. In the approach we used several Radiance programs in order to compute the incoming radiation landing on the manikin with high accuracy, even through a complex fenestration system. The

Gendaymtx tool generates a sky matrix with luminance values based on direct and diffuse component of the solar radiation using the Perez distribution, plus the Analemma matrix that generates the sun matrix. Rfluxmtx computes the daylight matrixes taking into account sky conditions, scene geometries, and material properties. Dctimestep is used for the matrix multiplication and a modified version of rmtxop is used to convert RGB output file into irradiance [W/m^2]. The manikins tested in this paper are defined by a sensor point placed at the centroid of each mesh face and oriented with a normal perpendicular to the surface centroid. Each sensor captures, for that specific portion of the body, the total solar radiation ($E_{solar,i}$) taking into account all the components of solar radiation (diffuse, reflected and direct).

Long wave MRT - EnergyPlus simulation
Simultaneously, an energy simulation using EnergyPlus can be run in order to calculate the air temperature, humidity and surface temperatures based on the scene properties described in Section 2.2. EnergyPlus' basic output gives the longwave MRT for one point placed in the center of the room. Given that the analyses are focused on the area close to the façade, we decided to compute the longwave MRT for six specific positions in the space located in the first 3 m adjacent to the façade, resulting in a spacing of 0.5 m. The longwave MRT is computed considering the surface temperatures of walls, glazed surfaces and the corresponding view factor for the exact user position, employing the method described in [11]. By adding the hourly MRT to the hourly ΔMRT obtained from the Radiance simulation, it is possible to compute the adjusted MRT with the SolCal method described in ASHRAE 55 appendix C for the performance approach. Finally, the PVM model is fed with the adjusted MRT to assess the thermal comfort and the percentage of potentially dissatisfied people.

Python Script
The Python script has two main functions; first computing the Effective Radiant Field (ERF), shortwave MRT, and ARD for each manikin in the space; second combining the shortwave MRT with the long wave MRT to calculate the adjusted MRT. In the Radiance section of the script, for each hour of the year we first multiply the $E_{solar,i}$ for each point by the equivalent area of the mesh to determine the total radiation on each surface. We then sum the radiation for all the surfaces to determine the total radiation falling on the body. Finally, by dividing the total radiation by the total body area, it is possible to calculate hourly the incoming radiation rate for the whole body (E_{solar}) (W/m^2). Using the formulas described by Arens [2], we compute the hourly ERF and ΔMRT for each manikin in the space and finally, we implement the ARD definition described in 2.4. The script embedded in Grasshopper generates graphs and heat map visualizations automatically.

2.2 Scene and Parameters
The simulated model uses in this simulation employs the same geometry as the ASHRAE BESTEST (see Figure 2) office space [7] fully described in Zani's paper for its optical

and thermal properties [20]. In order to guarantee a thermally neutral starting condition, an ideal HVAC has been modeled with a $T_{heating} = 20$ °C, $T_{cooling} = 26$ °C and minimum relative humidity equal to 30%. For the assessment of the PMV, the following standard values were used during the year: air flow speed of 0.1 m/s, users' metabolic rate of 1.2 met, and a dynamic clothing level based on outdoor temperature [17]. We tested three different façade configurations. Starting with classic insulated glazing units with two different values of solar transmittance, respectively 60% (low-e coating) and 28% (solar control coating). Second, a CFS with medium-low shade density obtained by coupling a glazing unit with 52% solar transmittance with static external louvers. The third configuration was a CFS with high shade density with geometry inspired by NMAAHC museum.

2.3 Spatial Mapping
In comparison with daylight performance metrics, a metric to assess the effective radiant field (ERF) and ΔMRT for the human body requires more than a typical sensor point every 0.45 m as required for LEED simulation and described in LM-83-12. In order to accurately calculate the intensity and direction of solar radiation landing on the occupant, it is necessary to use a more refined array of sensors. As presented in Zani et al. research work [20], a high-resolution manikin with 363 meshes combined with an accurate sky definition is able to fully capture the spatial complexity of the problem and accurately determines the change in MRT due to direct solar radiation. However, in order to create a more flexible framework that is able to investigate the performance of the façade independent of the position and orientation of the occupant, is necessary to extend the analysis to a grid of locations and remove the directionality of the manikin. A simplification of the manikin has been necessary in order to reduce the calculation time and create a non-directional representation. Starting from the high resolution (HR) manikin with 363 meshes described in [20], we tested a medium resolution (MR) with 120 meshes and a low resolution (LR) with 30 meshes, while maintaining the same total area. As described in Figure 3, we tested the accuracy and calculation analysis time of the simplified manikins (MR and LR) against the high-resolution one (HR), comparing the ΔMRT hourly values for the entire year with three different façade configurations. First, we compared the three manikins in a scene without a shading system (No shade).
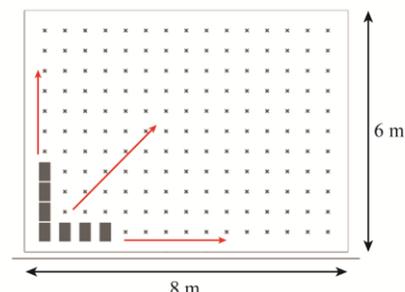

Figure 2. Office space configuration (ASHRAE BESTEST) and spatial distribution of manikins (red arrows).

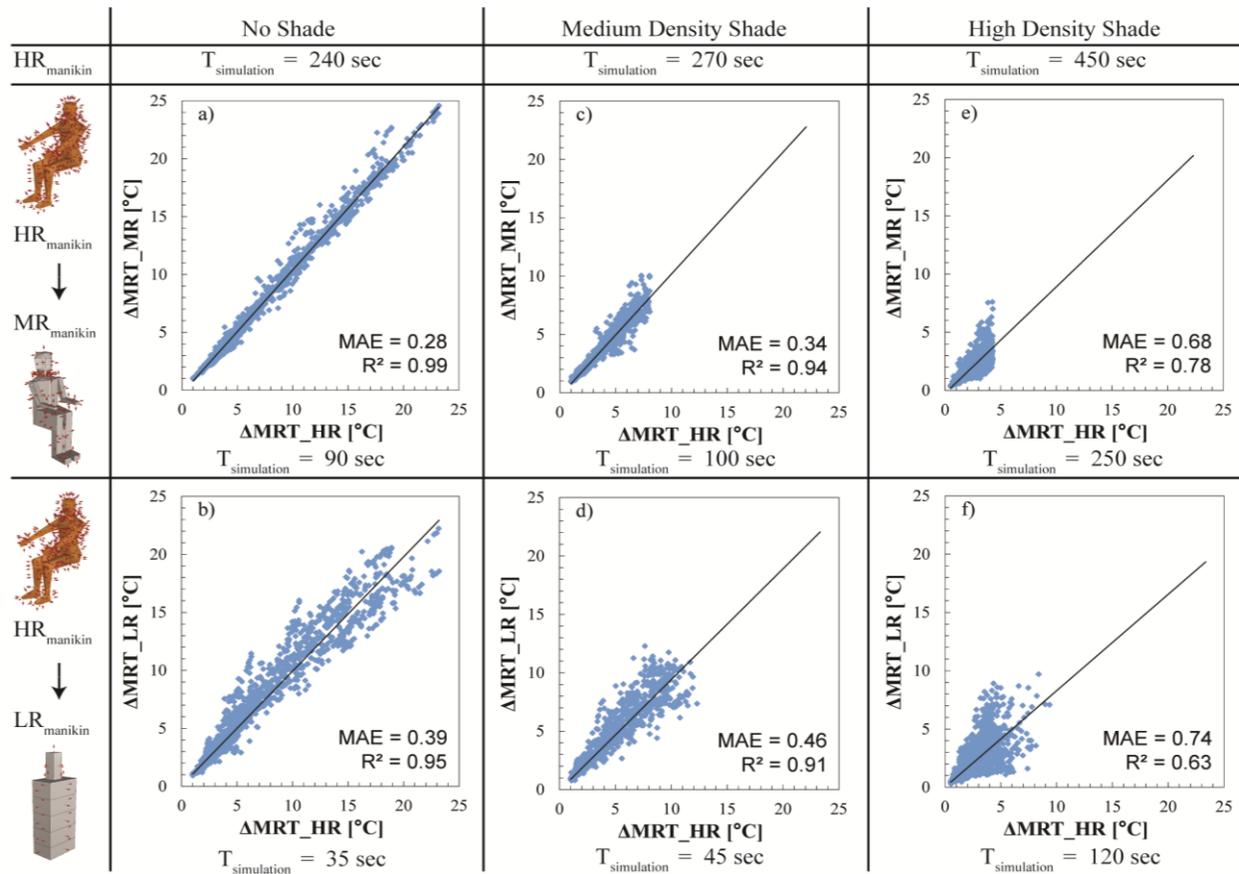|	No Shade	Medium Density Shade	High Density Shade
HR$_{manikin}$	T$_{simulation}$ = 240 sec	T$_{simulation}$ = 270 sec	T$_{simulation}$ = 450 sec

Figure 3. Accuracy and computational time comparison between manikins resolution for three different shading density.

As shown in Figure 3 in the first column, decreasing the number of calculation points does not affect the accuracy of the simulation, with a coefficient of determination (R^2) equal to 0.99 and 0.95 for the simplified manikins and a mean absolute error smaller than 0.4 °C. Meanwhile, we achieved a decrease of calculation time of up to 85% from 240 to 35 s. In the second comparison, we introduced a medium density solar shading system with external louvers characterized by a depth of 0.3 m and a spacing of 0.3 m. As expected, we had a decrease in the explained variance given the coarser meshes with a reduction in R^2 respectively of 0.05 and 0.04 compared to the "No Shade" case. In particular, in the range of ΔMRT between 2 and 5 °C that represents the tolerable range in the thermal comfort zone, the accuracy remains high with a MAE less than half degree. In addition, with a medium density shading system, we were able to reduce the simulation time by 80-85%. Finally, with a high-density solar screen, the scatter-plot graphs in the third column show a larger deviation of results. Both the simplified manikins present a coefficient of determination lower than 0.9, set as a threshold for this analysis, respectively 0.8 for MR and 0.63 for LR manikin.

A visual inspection of the data and the residuals shows that the linear model assumptions are satisfied for the case with no shade and medium density shade. For the high-density shade, there is clear heteroscedasticity of the data, indicating a larger uncertainty and lower reliability of the errors of the linear model. Given that the objective of these linear regressions is not the prediction of a dependent variable but the assessment of a model, we think that an adjustment (e.g., a Box-Cox transformation) is not needed. Based on the results shown following tests of the framework the LR manikin will be used only with simple glazing and medium shading density configurations.

2.4 Annual Discomfort Radiation Index
The Annual Discomfort Radiation Index (ADR) is based on the concept of annual metric like Daylight Autonomy (DA) [4]. The ADR index is defined as the percentage of the occupied hours (from 8 to 18) of the year when the ΔMRT for each manikin position (see Figure 2) is over the threshold of 4 °C.

$$ARD = \frac{\sum_j (wf_i \cdot t_i)}{\sum_j t_i} \quad wf_i = 1 \; if \; \Delta\text{MRT}_i > 4°\text{C}$$

Where the t_i is each occupied hour in a year; and the ΔMRT_i is the hourly value of shortwave mean radiant temperature for each point of the grid. We selected the 4 °C ΔMRT threshold for ARD because, starting from a neutral thermal condition with a PMV value between -0.1 and 0.1; an MRT increment of this magnitude produces a shift in the occupant's comfort zone, moving the occupant outside the boundaries with a higher PMV, causing slightly warm

conditions (see figure 4). The underlying definition of the ARD index is the assumption that the overall space, and in particular the area close to the façade, is properly thermally controlled by the HVAC system. Specifically, the HVAC system is able to maintain the comfort conditions of occupants when the sun is not striking in the space. The actual definition has not been evaluated for other comfort methods such as the adaptive method [6]. Given the variability in the thermal comfort range based on façade configuration, space activities space subdivision, and sensibility of mechanical systems, the ΔMRT threshold can be adjusted on a case by case basis. By deliberately only using ΔMRT in the calculation of the ARD metric, the results are decoupled from the HVAC system. This allows designers to isolate the effect of direct solar radiation on the comfort of occupants across the spaces they design, providing specific insight that was unavailable before.
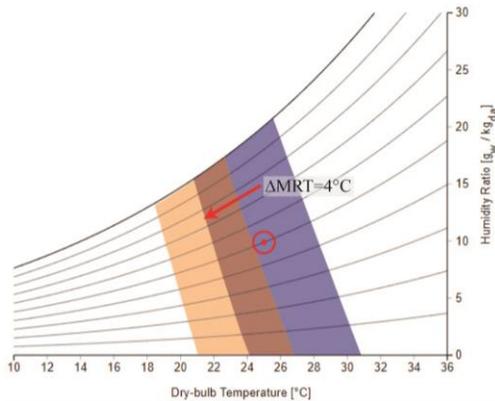

Figure 4. Comfort zone shift due to the increment of MRT caused by incoming solar radiation.

To visualize the ARD index the python script generates two outputs (see Figure 5). The first part (on the left) is an RGB-color scheme that can be used to highlight areas on the floor plan that experience uncomfortable thermal condition over the year. The spatial map reveals the percentage of occupied hours where the ΔMRT is greater than 4°C. A number of uncomfortable hours, in the first three meters of the space, larger than 10% [5] is considered unacceptable.
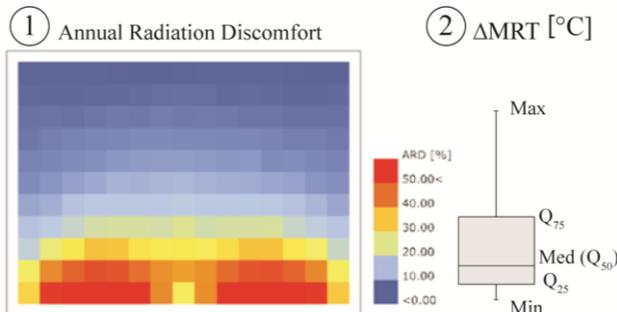

Figure 5. Framework results overview: ARD spatial color map (on the left) and ΔMRT intensity distribution (on the right).

In addition to the spatial heat map, the python script outputs a box-plot chart to visualize the magnitude of ΔMRT in the first three meters from the façade, considered by ASHRAE 55 in the prescriptive approach as a buffer of unused area in order to guarantee occupants' thermal comfort. In particular, looking at this plot, designers can easily visualize the statistical distribution of ΔMRT during the year and extract median, extreme values. Coupling the two visualizations, we have a spatial, temporal and magnitude understanding of the phenomena and an additional instrument to assess the façade performance.

3 APPLICATION OF ANNUAL DISCOMFORT RADIATION INDEX TO INFORM DESIGN - RESULTS

All the preliminary analyses, simplifications, and assumptions presented so far, have as a final goal the development of a framework that can support the design decision-making side by side with the traditional daylight metrics as DA, sDA, UDI, and ASE. In order to demonstrate the framework we tested and analyzed three façade configurations using the test room and parameters presented in paragraph 2.2. The three façade systems tested, in summary, were two glazing system without shading and with a solar transmittance of 60% and 28% (labeled T60 and T28), and one glazing system with solar transmittance of 52% with shading louvers (labeled T52+L). As indoor conditioning was imposed continuously through the year, additional discomfort for the user would be caused by the increase of MRT due to shortwave radiation. The overall performance criterion for the façade systems takes into account ARD, ΔMRT range, DA_{300}, $UDI_{300-3000}$ and $ASE_{1000Lux, 250h}$. In the second part, we assessed the influence of ΔMRT on the PMV in the first three meters of the floorplate adjacent to the façade in order to understand the occupant's thermal sensation with and without the effect of solar radiation.

3.1 Annual Discomfort Radiation and Daylight

Figure 6 shows the false-color and the box-plot visualization for the three cases analyzed. In the office space with a typical low-e glass (T60_NoShade) the number of uncomfortable hours due to incoming solar radiation falling on building occupants reach peaks of 50-60% in the first 2 meters and around 30-40% in the following meter. As shown in the box-plot representation for T60_NoShade, the median value in the first 3 m is 3.2 °C; close to the critical threshold of 4 °C. In addition, we note a wide variation in the upper quartiles, with a peak of 25 °C. By replacing the glass with high-performance glazing with a solar transmittance of 28% (T28_NoShade), we were able to reduce the number of uncomfortable hours near the façade by 15% with a peak reduction of 30-40% in the first meter.

Case	DA [%h]	UDI [%h]	ASE [%h]	ARD$_{3m}$ [%h]
T60	86.6	69.6	42	28
T28	80.5	74.2	40	15
T52+L	83.9	77.9	13	10

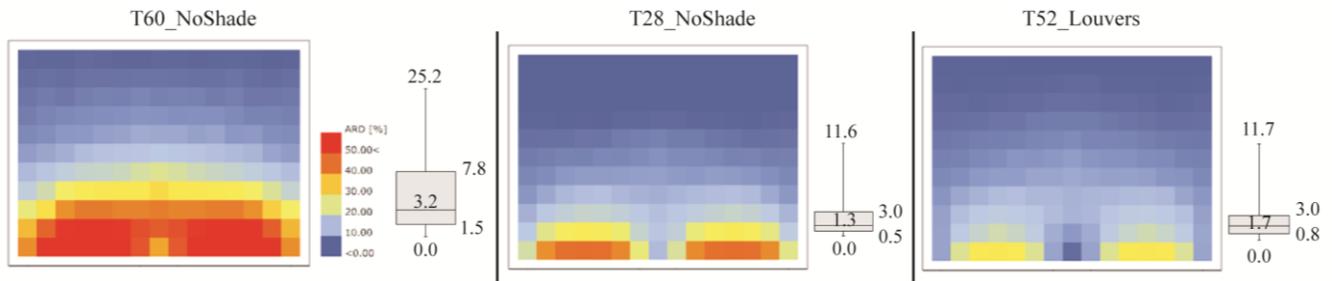**Table 1.** Daylight performance scores and average ARD.

Figure 6. False color plots of Annual Radiation Discomfort (ARD) and box-plot for ΔMRT.

We achieved a consistent reduction also in the peak and median values of ΔMRT. In addition, from the boxplot, we can understand that 75% of ΔMRT values are below the critical threshold of 4 °C. Finally, coupling a low-e glass with external louvers (T52_Louvers), we achieve a further improvement in the "thermal" performance with an average value of ARD in the first three meters equal to 10% and a peak of 25% in the first meter. We found a similar distribution in ΔMRT values with the T28_NoShade, with a slight increase in the median value from 1.3 °C to 1.7 °C.

Table 1 shows for the same cases presented for ARD, the overall daylight performance. Considering the three metrics, we can understand that the glazing plus shading system configuration (T52_Louvers) presents the best daylight performance with the highest level of UDI and the lowest ASE compared to the glazing solutions without shading. In particular, the proposed solution is able to maintain the same level of Daylight Autonomy and reduce the amount of overlit hours. Taking into account both thermal and daylight performance, the T52_Louvers façade configuration performs better, decreasing the number of uncomfortable hours near the glazing while maintaining a good level of illuminance across the space.

3.2 ARD and the Influence on Interior Comfort (PMV)

In addition to the daylight and comfort parameters described above, we also calculated the adjusted PMV for point in time and annual analyses by coupling the outputs from Radiance (ΔMRT) and EnergyPlus (MRT).

Figure 7 shows the PMV values in the office space considering the effect of shortwave radiation on the 21st of December at 9:00 for two different glazing solutions. With 60% solar transmittance, occupants in more than half of the space may experience warm or extremely warm thermal sensation. Additionally, occupants in the other half of the space not directly impacted by direct radiation experience discomfort conditions. With the same outdoor conditions, a solar control glass can guarantee a more comfortable space. PMV over the comfort range is experienced only in the first couple of meters of the floor plate adjacent to the façade and localized only in the portion struck by direct sun. Figure 8 shows the annual variance of PMV and PMV adjusted to include direct solar radiation for the area within the first three meters of the façade for the same three façade configuration assessed before.
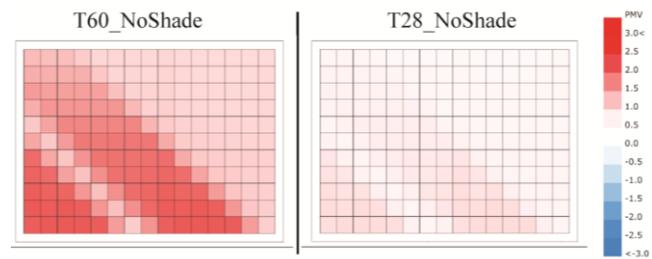

Figure 7. Point in time false color visualization of PMV.

As expected, the glazing system with high solar transmittance (T60_NoShade) that presents the highest ARD also has the wider range in adjusted PMV values. For the T60_NoShade conditions without considering the effect of the incoming shortwave radiation, the median PMV value is slightly above 0. By adding the ΔMRT, the median value rises to 1 and for 50% of the time occupants of the area close to the window experience intolerable thermal conditions.

Installing solar control glass or external louvers as shading devices effectively show their effectiveness in decreasing negative thermal comfort conditions. The variance on the thermal sensation after ΔMRT was considered, has been substantially reduced compared to the low-e glazing. Both T28_NoShade and T52_Louvers show a maximum PMV value equal to 2 and a median value close to neutral. More than 50% of the values (first and third quartile) are included in the PMV comfort zone between -0.5 and 0.5.
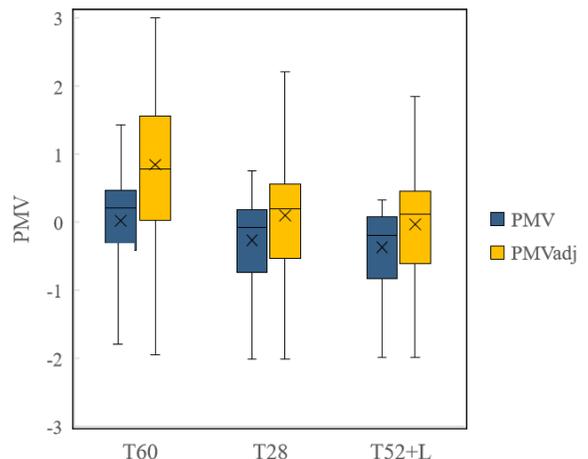

Figure 8. PMV and PMV adjusted variance influenced by façade configuration.

4 DISCUSSION

The results presented in the previous section show that it is feasible to assess the discomfort due to solar radiation landing on occupants across a floor plan. The ARD index calculated using ΔMRT can be used to compare and optimize façade systems to reduce the influence of incoming shortwave radiation on comfort from the first stage of design without the need of complex energy simulations. Energy simulations can be added in subsequent phases to fully understand the overall thermal performance of the system and introduce PMV calculation. The combined results visualization presented in Figure 5 clearly shows the spatial distribution of critical areas of concern and the magnitude of the phenomenon and facilitate the interpretation of results to inform the design process. In the preliminary tests presented in 2.3, we observed a significant variation in the accuracy of the results due to the sensor points density and the complexity of the shading system. For this reason, we suggest selecting the manikin-based on the detail level of the scene and the accuracy required.

The case study results show that significant improvements can be achieved using specific design solutions like solar control glass or external shading systems. ARD results effectively complement classic daylight grid-based metrics, creating a set of holistic metrics that are able to fully describe the performance of a façade system.

From preliminary comparison, between ARD and ASE, it appears that ASE tends to overestimate the amount of space and hours in which occupants are potentially in discomfort condition. Additional comparisons will be carried out in following research studies.

5 CONCLUSIONS AND FUTURE DEVELOPMENTS

This paper introduces a new analysis framework to calculate the number of discomfort hours due to by solar radiation landing directly on occupants. The flexible workflow can be used from the early stages of design or for more detailed analysis when coupled with energy simulations. As shown in the tests, the new Annual Radiation Discomfort (ARD) metric can be employed to estimate the performance of different shading strategies, reduce unused space near the façade caused by increased temperatures, or control roller shade deployment when combined with daylight performance metrics. Furthermore, the ARD metric allows designers to predict the thermal sensations of occupants across the floor at every hour of the year, using a single simulation with the appropriate manikin definition selected based on the complexity of the application.

Although direct solar radiation falling on the user might occur only a few hours during the day, it can generate uncomfortable thermal condition throughout the year that cannot be offset by a HVAC system. This may increase the hours of discomfort experienced by the occupants, potentially leading to the decay of human health and loss of productivity or learning proficiency. Having a framework and a metric that take into account the effect of direct shortwave radiation on comfort can increase the awareness of the issue and help practitioners design more thermally comfortable spaces.

The framework and analyses described in the paper open the way to new research questions and provide the opportunity to further improve the accuracy and enhance the capacity of the tool:

- Test different manikin-sensor points density to increase the accuracy of simulations for highly complex shading system.

- Investigate the implementation of Bidirectional Scattering Distribution Function (BSDF) in simulations. Given the required spatial resolution, Klems and Tensor-tree BSDF can be tested.

- Thorough comparisons between ARD, UDI and ASE to investigate possible similarities.

- Release a series of open-source Grasshopper components.

- Introduce, for high accuracy simulation, the assessment of overall and local thermal sensations using Machine Learning techniques. Time-series algorithms can be applied in order to make an accurate prediction about what should be the right temperature to apply in a particular room at a specific time.

REFERENCES

1. Akimoto, T., Tanabe, S., Yanai, T., & Sasaki, M. (2010). Thermal comfort and productivity - Evaluation of workplace environment in a task conditioned office. *Building and Environment*, *45*, 45–50.

2. Arens, E., Hoyt, T., Zhou, X., Huang, L., Zhang, H., & Schiavon, S. (2015). Modeling the comfort effects of short-wave solar radiation indoors. *Building and Environment*, *88*, 3–9.

3. Bessoudo, M., Tzempelikos, A., Athienitis, A.K., & Zmeureanu, R. (2010). Indoor thermal environmental conditions near glazed facades with shading devices - Part I: Experiments and building thermal model. *Building and Environment*, *45*(11), 2506–2516.

4. Carlucci, S., Causone, F., De Rosa, F., & Pagliano, L. (2015). A review of indices for assessing visual comfort with a view to their use in optimization processes to support building integrated design. *Renewable and Sustainable Energy Reviews*, *47*(7491), 1016–1033.

5. Carlucci, S., Pagliano, L., & Sangalli, A. (2014). Statistical analysis of the ranking capability of long-term thermal discomfort indices and their adoption in optimization processes to support building design. *Building and Environment*, *75*, 114–131.

6. De Dear R.J., Brager G. (1998) Developing an Adaptive Model of Thermal Comfort and Preference, Am. Soc. Heating, Refrig. Air Cond. Eng. Inc., Macquarie Res. Ltd. 4106.

7. Henninger, R.H., & Witte, M. J. (2004). EnergyPlus testing with ANSI/ASHRAE standard 140-2001 (BESTEST). *U.S. Department of Energy*

8. Hoyt, T., Schiavon, S., Piccioli, A., Cheung, T., Moon, D., Steinfeld, K. (2017). CBE Thermal Comfort Tool. Retrieved from http://comfort.cbe.berkeley.edu/

9. Konis, K. (2013). Evaluating daylighting effectiveness and occupant visual comfort in a side-lit open-plan office building in San Francisco, California. *Building and Environment*, *59*, 662–677.

10. Konis, K., & Selkowitz, S. (2017). *Effective Daylighting with High-Performance Facades*. Springer.

11. Mackey, C., Baranova, V., Petermann, L., Menchaca-Brandan, A. (2017) Glazing and Winter Comfort Part 2 : An Advanced Tool for Complex Spatial and Temporal Conditions, Build Sim., 2317–2325.

12. Marino, C., Nucara, A., & Pietrafesa, M. (2017). Thermal comfort in indoor environment: Effect of the solar radiation on the radiant temperature asymmetry. *Solar Energy*, *144*, 295–309.

13. Marino, C., Nucara, A., Pietrafesa, M., & Polimeni, E. (2017). The effect of the short wave radiation and its reflected components on the mean radiant temperature: modelling and preliminary experimental results. *Journal of Building Engineering*, *9*, 42–51.

14. Sadeghipour M., Pak M. (2013). Ladybug: a Parametric Environmental Plugin for Grasshopper To Help Designers Create an Environmentally-Conscious Design, 13th Conf. Int. Build. Perform. Simul. Assoc.

15. Reinhart, C.F., Mardaljevic, J., & Rogers, Z. (2006). Dynamic daylight performance metrics for sustainable building design. *LEUKOS* - J. Illum. Eng. Soc. North Am. 3

16. Reinhart, C.F., & Walkenhorst, O. (2001). Validation of dynamic RADIANCE-based daylight simulations for a test office with external blinds. *Energy and Buildings*, *33*(7), 683–697.

17. Schiavon, S., & Lee, K.H. (2013). Dynamic predictive clothing insulation models based on outdoor air and indoor operative temperatures. *Building and Environment*, *59*, 250–260.

18. Wargocki, P., Frontczak, M., Schiavon, S., Goins, J., Arens, E., & Zhang, H. (2008). Satisfaction and self-estimated performance in relation to indoor environmental parameters and building features. *10th Int. Conf. Heal. Build.* 1–7.

19. Wolfgang, K., Frenzel, C., Hiller, M., Muller, K. (2011). Simulation of thermal comfort in soccer stadia using Trnsys 17. *International Building Performance Simulation Association.*

20. Zani, A., Mainini, A.G., Cadena, J.D.B., Schiavon, S., & Arens, E. (2018). A New Modeling Approach for the Assessment of the Effect of Solar Radiation on Indoor Thermal Comfort. *Building Performance Analysis Conference and SimBuild.*